

# Universal non-exponential relaxation and memory effects in a fluid with non-linear drag

A. Patrón,<sup>1,\*</sup> B. Sánchez-Rey,<sup>2,†</sup> and A. Prados<sup>1,‡</sup>

<sup>1</sup>*Física Teórica, Universidad de Sevilla, Apartado de Correos 1065, E-41080 Sevilla, Spain*

<sup>2</sup>*Departamento de Física Aplicada I, E.P.S., Universidad de Sevilla, Virgen de África 7, E-41011 Sevilla, Spain*

(Dated: July 27, 2021)

We analyse the dynamical evolution of a fluid with non-linear drag, for which binary collisions are elastic, at the kinetic level of description. When quenched to low temperatures, the system displays a really complex behaviour. The glassy response of the system is controlled by a long-lived non-equilibrium state, and includes non-exponential, algebraic, relaxation and strong memory effects in the time evolution of its kinetic temperature. Moreover, the observed behaviour is universal, in the sense that the time evolution of the temperature—for both relaxation and memory effects—falls onto a master curve, regardless of the details of the experiment. Our theoretical predictions are checked against simulations of the kinetic equation, and an excellent agreement is found.

*Introduction.*— Glassy behaviour is typically associated with systems with many strongly interacting units, which give rise to a complex energy landscape with multiple minima separated by barriers [1–3]. The typical phenomenology of glassy systems includes, among other aspects, strongly non-exponential relaxation [4–15]. The latter facilitates the emergence of memory effects like the Kovacs hump, in which the relevant physical quantity displays a non-monotonic behaviour—despite initially having its equilibrium value [16–30]. The Kovacs effect comes about because the evolution of the system does not only depend on the value of the thermodynamic (or hydrodynamic) variables but also on additional ones, the values of which are determined by the way the state has been prepared—i.e. on how the system has been previously aged [11, 13, 21, 31–38].

Aging is also connected with the Mpemba effect [39], which has recently been observed in spin glasses [40]. In the Mpemba effect, the initially hotter sample cools sooner and the relaxation curves thus cross at a certain time. Only very recently has it been theoretically investigated, both from a stochastic thermodynamics [41–44] and a kinetic theory [45–51] approach. In the former, the crossing is described in terms of the Kulback-Leibler distance to equilibrium. In the latter, the crossing is described in terms of the kinetic temperature. Therefore, the kinetic approach is closer to the experimental situation and has been successful in showing that the Mpemba effect may emerge even in very simple systems like granular gases [45–50]. Notwithstanding, the following crucial question remains unanswered: How does the system have to be aged for the Mpemba effect to emerge? This is one key question that we solve in this Letter.

Specifically, we analyse a very general model for a fluid with non-linear drag, which is rooted in the theory of non-linear Brownian motion [52]. It can be visualised

as a mixture of two fluids: a fluid of Brownian particles moving in a background fluid acting as a thermal bath. When the masses of the Brownian and the background fluid particles are comparable, the drag force felt by the former is non-linear in their velocities [53, 54]. This model has been recently shown to accurately describe the dynamics of ultracold gases, such as an ensemble of <sup>133</sup>Cs atoms moving in a dilute background cloud of <sup>87</sup>Rb atoms. Despite the very low temperatures involved, in the  $\mu\text{K}$  range, the low density makes it possible to describe the system with the tools of classical statistical mechanics, namely the model that we employ throughout [55].

Although the energy landscape of the Brownian particles is very simple, its energy being only kinetic, we show that there appears a strong non-exponential relaxation when the system is quenched to low enough temperatures. Moreover, this non-exponential relaxation is universal in the sense that, after a suitable rescaling of the variables, it is independent of the initial and final temperatures, and also of the degree of non-linearity. Interestingly, this non-exponential relation is closely linked to the existence of a long-lived non-equilibrium state (LLNES). Therein, the higher cumulants of the velocity distribution function are basically time-independent while the temperature is algebraically decaying. Besides, the LLNES rules the emergence of strong memory effects. In particular, we investigate both the Mpemba and the Kovacs effects, which are also shown to display universal features.

*The model.*— Our system consists of  $d$ -dimensional hard spheres of mass  $m$ , diameter  $\sigma$ , and number density  $n$  (the Brownian particles), immersed in a uniform and isotropic fluid at equilibrium with temperature  $T_s$  (the background fluid). The one-particle velocity distribution function (VDF)  $f(\mathbf{v}, t)$  for the Brownian particles satisfies the Enskog–Fokker–Planck (EFP) equation

$$\partial_t f(\mathbf{v}, t) = \frac{\partial}{\partial \mathbf{v}} \cdot \left[ \zeta(v) \left( \mathbf{v} + \frac{k_B T_s}{m} \frac{\partial}{\partial \mathbf{v}} \right) f(\mathbf{v}, t) \right] + J[\mathbf{v}|f, f]. \quad (1)$$

The terms on the right hand side of the EFP equation stem from different interactions. That among the

\* apatron@us.es

† bernardo@us.es

‡ prados@us.es

Brownian and the background fluid particles gives rise to both the nonlinear drag force  $\mathbf{F}_{\text{drag}} = -m\zeta(v)\mathbf{v}$  and the white-noise stochastic force  $\mathbf{F}_{\text{wn}}$  with correlation  $\langle \mathbf{F}_{\text{wn}}(t)\mathbf{F}_{\text{wn}}(t') \rangle = 2mk_B T_s \zeta(v)\delta(t-t')$ , where  $k_B$  is Boltzmann's constant. On the other hand, the Enskog collision operator accounts for the collisions among the mutually interacting Brownian particles [56]. The variance of the stochastic force follows from the fluctuation-dissipation relation [52] and ensures that the only stationary solution of Eq. (1) is the equilibrium Maxwellian,  $f_s(\mathbf{v}) = n(2\pi k_B T_s/m)^{-d/2} \exp(-mv^2/2k_B T_s)$ .

In this Letter, we consider a physical situation in which the masses of the Brownian and the background fluid particles are comparable. The drag force is thus nonlinear in the velocity [53–55],

$$\zeta(v) = \zeta_0 \left( 1 + \gamma \frac{mv^2}{k_B T_s} \right), \quad (2)$$

where  $\zeta_0$  is constant and  $\gamma$  is the non-linearity parameter. There are two characteristic times in this system: the time over which the Brownian particles feel the drag due to the background fluid  $\zeta_0^{-1}$ ,  $\zeta_0^{-1} \propto T_s^{-1/2}$  [53–55], and the time between collisions among the Brownian particles  $\tau_s$ , also  $\tau_s \propto T_s^{-1/2}$  [47, 56]. The relative relevance of the non-linear drag force and the Brownian-Brownian collisions is thus measured by the dimensionless parameter  $\xi = \zeta_0 \tau_s$ , which is independent of  $T_s$ . For  $\xi \gg 1$ , basically the collisions among the Brownian particles can be neglected, whereas the latter become dominant in the opposite limit  $\xi \ll 1$  [57]. In addition, it is convenient for our purposes to define dimensionless variables for temperature,  $\theta = T/T_s$ , and time,  $t^* = \zeta_0 t$ —we drop the asterisk in the following to simplify the notation.

To account for the observed behaviour, we have to consider an *extended* Sonine expansion of the VDF, in which both the fourth cumulant or excess kurtosis

$$a_2 \equiv -1 + \frac{d}{d+2} \frac{\langle v^4 \rangle}{\langle v^2 \rangle^2} \quad (3)$$

and the sixth cumulant

$$a_3 \equiv 1 + 3a_2 - \frac{8}{d(d+2)(d+4)} \frac{\langle v^6 \rangle}{\langle v^2 \rangle^3} \quad (4)$$

are retained. Within this approximation, the following

evolution equations for  $(\theta, a_2, a_3)$  hold [58] [56, 59],

$$\begin{aligned} \dot{\theta} &= 2(1-\theta) [1 + \gamma(d+2)\theta] - 2\gamma(d+2)\theta^2 a_2, & (5a) \\ \dot{a}_2 &= 8\gamma(1-\theta) - \left[ \frac{4}{\theta} - 8\gamma + 4\gamma(d+8)\theta + \frac{8(d-1)}{d(d+2)} \frac{\sqrt{\theta}}{\xi} \right] a_2 \\ &\quad + 2 \left[ 2\gamma\theta(d+4) + \frac{(d-1)}{d(d+2)} \frac{\sqrt{\theta}}{\xi} \right] a_3, & (5b) \\ \dot{a}_3 &= 12 \left[ -4\gamma + 6\gamma\theta + \frac{(d-1)}{d(d+2)(d+4)} \frac{\sqrt{\theta}}{\xi} \right] a_2 \\ &\quad + 6 \left[ 4\gamma - \frac{1}{\theta} - \gamma\theta(d+14) - \frac{(d-1)(4d+19)}{2d(d+2)(d+4)} \frac{\sqrt{\theta}}{\xi} \right] a_3. & (5c) \end{aligned}$$

The equilibrium solution of this system is  $\theta_s = 1$  and  $a_2^s = a_3^s = 0$ , since the equilibrium VDF is Gaussian.

For linear drag,  $\gamma = 0$ , the temperature obeys the closed Newton's law of cooling,  $\dot{\theta} = 2(1-\theta)$ . Therefore, it relaxes exponentially to equilibrium,  $\theta(t) = 1 + [\theta_i - 1]e^{-2t}$ , for all  $\theta_i \equiv \theta(0)$ . Moreover, the VDF remains Gaussian,  $a_2(t) = a_3(t) = 0$ . For non-linear drag, since typically  $\gamma \lesssim 0.1$  [60], one might guess that both the deviations from the exponential relaxation and the Gaussian VDF should be small: we show in the following that this intuition is utterly wrong. There emerges a strong non-exponential relaxation together with quite large, time- and  $\gamma$ -independent, cumulant values when the system is quenched to a low temperature.

*Quench to low temperatures.*— If the initial and final temperatures are of the same order,  $\theta_i = O(1)$ , mild deviations from the exponential behaviour are observed [56]. Here, we are interested in the limit  $\theta_i \gg 1$ , i.e. a quench to a low temperature. Therein, the evolution equations for the temperature  $\theta$  and the cumulants  $a_2$  and  $a_3$  simplify to [56]

$$\frac{dY}{ds} = -2(d+2)Y^2(1+a_2), \quad (6a)$$

$$\frac{da_2}{ds} = -4Y [(d+8)(a_2 - a_2^r) - (d+4)(a_3 - a_3^r)], \quad (6b)$$

$$\frac{da_3}{ds} = -6Y [-12(a_2 - a_2^r) + (d+14)(a_3 - a_3^r)], \quad (6c)$$

where  $Y \equiv \theta/\theta_i$  and  $s \equiv \gamma\theta_i t$ . Above,  $a_2^r$  and  $a_3^r$  are reference values for the cumulants, specifically

$$a_2^r = -\frac{2(d+14)}{d^2 + 10d + 64}, \quad a_3^r = -\frac{24}{d^2 + 10d + 64}, \quad (7)$$

which are independent of  $\gamma$ . For  $d = 2$ ,  $a_2^r \simeq -0.36$  and  $a_3^r \simeq -0.27$ .

*Universal non-exponential relaxation.*— The right hand side of Eq. (6) does not depend on  $\gamma$ , which has been absorbed in the time scale  $s$ . The relaxation of the system is universal in the following sense: all the relaxation curves of the temperature should be superimposed when  $Y = \theta/\theta_i$  is plotted against  $s = \gamma\theta_i t$ . This universality is

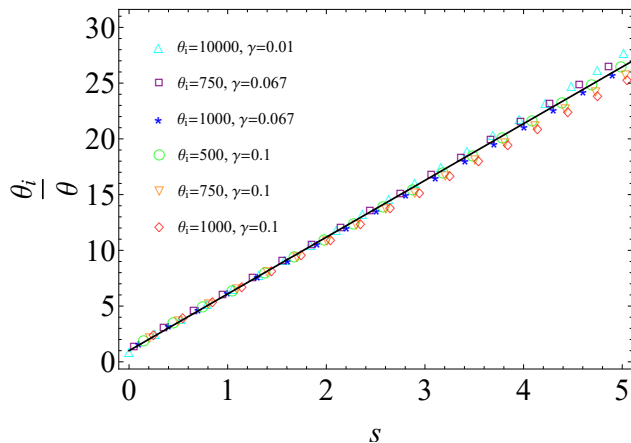


FIG. 1. Relaxation after a quench to a low temperature. Specifically, we plot  $1/Y = \theta_i/\theta$  as a function of the scaled time  $s = \gamma\theta_i t$ . Data from DSMC correspond to parameter pairs  $(\gamma, \theta_i)$ , as specified in the legend,  $d = 2$  and  $\xi = 1$ . Also plotted is the theoretical prediction in Eq. (8) (solid line). The linear behaviour of  $1/Y$  means that the temperature relaxes algebraically, basically as  $t^{-1}$ .

checked in Fig. 1, in which several relaxation curves for the temperature are shown. They have been obtained by numerically solving the kinetic equation by the Direct Simulation Monte Carlo (DSMC) method [61, 62]. Specifically, we plot  $1/Y$  versus  $s$ , for values of  $\gamma$  and  $\theta_i$  such that  $0.01 \leq \gamma \leq 0.1$  and  $50 \leq \gamma\theta \leq 100$ , respectively. A clear linear behaviour arises, i.e.  $Y(s)$  shows a very slow algebraic decay, basically proportional to  $s^{-1}$  or, equivalently,  $t^{-1}$ . A similar behaviour has been recently found for the relaxation dynamics of several glass-forming models to their inherent structures [15].

This strongly non-exponential relaxation can be theoretically understood in the following way: the cumulants rapidly tend (over the  $s$  scale) to their reference values  $a_2^r$  and  $a_3^r$  [56]. Setting  $a_2 = a_2^r$  in Eq. (6a), we get

$$Y(s) = Y_{\text{alg}}(s) \equiv \frac{1}{1 + 2(d+2)(1 + a_2^r)s}. \quad (8)$$

This theoretical prediction is also plotted in Fig. 1, where it is neatly seen that the agreement with the numerical results is excellent.

The validity of Eq. (8) over a wide time range means that the system remains in a LLNES for most of the relaxation in the low-temperature quench. Over this non-equilibrium state, the cumulants  $a_2$  and  $a_3$  equal their reference values (7), whereas the temperature decays algebraically following Eq. (8). This state only breaks for very long times, for which  $1/Y$  does not diverge but saturates to its equilibrium value [63].

*Memory effects.*— The just described non-exponential relaxation opens the door to the emergence of strong memory effects. We start the analysis with the Mpemba effect. The cooling rate increases with the excess kurtosis  $a_2$ , as follows from Eq. (5) [64]. For the Mpemba effect

to emerge, the initially hotter sample (A, initial temperature  $\theta_{i,A}$ ) must cool faster than the initially colder one (B, initial temperature  $\theta_{i,B}$ ), i.e.  $a_{2i,A} > a_{2i,B}$ .

Here, not only do we show that for large enough difference  $\Delta a_{2i} \equiv a_{2i,A} - a_{2i,B}$  the Mpemba effect emerges, but (i) how to maximise the effect and (ii) how the system has to be previously *aged* to get such an initial preparation of the samples. In order to optimise the Mpemba effect,  $a_{2i,A}$  ( $a_{2i,B}$ ) must take its largest (smallest) possible value. Therefore,  $\dot{a}_2$  must vanish at the end of the aging time window. The analysis of this condition shows that the largest possible value of the excess kurtosis  $a_2^{\text{max}}$  is positive, proportional to  $\gamma$  and thus rather small, while its smallest possible value  $a_2^{\text{min}}$  is negative and basically equals the reference value  $a_2^r$  in Eq. (7) [56].

Thus, the Mpemba effect can be optimised in the following way. On the one hand, the initially colder sample B is prepared by quenching the molecular fluid from a very high temperature. With this process, we obtain a sample with  $a_{2i,B} = a_2^r$ , i.e. the minimum possible value. On the other hand, the initially hotter sample A is at equilibrium,  $a_{2i,A} = 0$ . This is the simplest, most practical—and also very close to optimal—choice [65]. These samples A and B are put in contact with a common thermal reservoir with a much lower temperature, so Eqs. (6) govern the evolution of our system for a long time and, in particular, are capable of describing the *universal* Mpemba effect observed. The initially hotter sample cools with  $a_2$  decreasing from zero towards  $a_2^r$ , i.e.

$$Y_A(s_A) = \frac{\theta_A(s_A)}{\theta_{i,A}} = f(s_A), \quad s_A = \gamma\theta_{i,A}t, \quad (9)$$

where  $f$  is a certain function, independent of  $\theta_{i,A}$ , the exact form of which is irrelevant for our discussion. The initially colder sample cools following Eq. (8), i.e.

$$Y_B(s_B) = \frac{\theta_B(s_B)}{\theta_{i,B}} = Y_{\text{alg}}(s_B), \quad s_B = \gamma\theta_{i,B}t. \quad (10)$$

The Mpemba effect takes place when  $\theta_A = \theta_B$  for some crossing time  $t_\times$ .

Figure 2 shows the strong Mpemba effect displayed by the system. Since both the  $Y$  and  $s$  variables depend on the initial conditions, we plot  $Y_B = \theta/\theta_{i,B}$  vs.  $s_B = \gamma\theta_{i,B}t$ . After defining the initial temperature ratio  $R_{AB} \equiv \theta_{i,A}/\theta_{i,B} > 1$ ,  $Y_A = Y_B/R_{AB}$  and  $s_A = R_{AB}s_B$ . Specifically, we consider one B sample, with  $\theta_{i,B} = 100$ , and four different A samples, with  $R_{AB} = 1.05, 1.1, 1.15, 1.2$ . Symbols correspond to DSMC simulations of the system and lines to the theoretical prediction stemming from Eqs. (6). The temperature curves cross at a certain time  $s_{B,\times}$ , which corresponds to  $t_\times$  in the original time scale,  $s_{B,\times} = \gamma\theta_{i,B}t_\times$ . For  $s_B > s_{B,\times}$ , the curve for the initially hotter sample lies below that of the initially colder. The strength of the Mpemba effect decreases with the initial temperature difference. However, it is neatly observed for the last case with 20 per cent initial temperature difference—and it is still present up to 40 per cent [56].

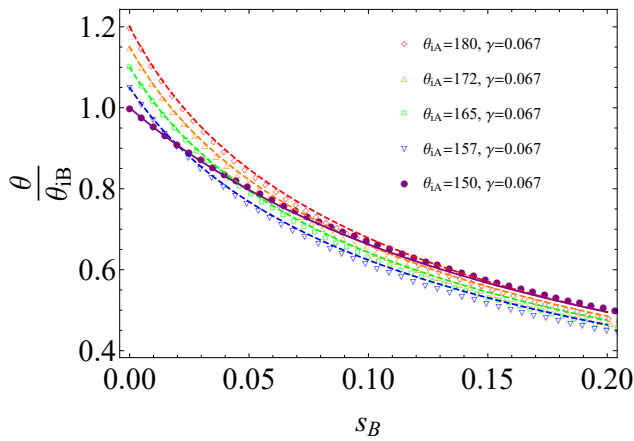


FIG. 2. Mpemba effect for different initial temperature ratios  $R_{AB}$ . Specifically, we consider four values of  $R_{AB}$ ,  $R_{AB} = 1.05, 1.1, 1.15$  and  $1.2$ , for  $\gamma = 0.1$ . Additional parameters employed are  $d = 2$  and  $\xi = 1$ . We plot  $\theta/\theta_{i,B}$  as a function of  $s_B$ , from the DSMC simulation and the theoretical prediction stemming from Eq. (6). The relaxation curve of the cold sample B (circles DSMC, solid line theory), starting from  $\theta_{i,B} = 100$  with  $a_{2i,B} = a_2^r$ , is crossed by the curves for the hot samples A (empty symbols DSMC, dashed lines theory), which start from  $\theta_{i,A} = R_{AB}\theta_{i,B}$  with  $a_{2i,A} = 0$  (i.e. at equilibrium).

The Mpemba effect is moreover universal in the following sense. Let us consider a fixed value of the initial temperature ratio  $R_{AB}$ , but different values of the non-linearity parameter  $\gamma$  and the initial temperatures  $\theta_{i,A}$  and  $\theta_{i,B}$ . If we plot  $\theta/\theta_{i,B}$  vs.  $s_B$ , all the curves corresponding to the colder temperatures superimpose, as Fig. 1 shows. Besides, also the curves corresponding to the hotter temperatures superimpose, because  $s_A = R_{AB}s_B$  and Eq. (9) entails  $\theta_A(s_B) = \theta_{i,A}f(R_{AB}s_B)$  or, equivalently,  $\theta_A(s_B)/\theta_{i,B} = R_{AB}f(R_{AB}s_B)$ . This is neatly shown in Fig. 3, where we have plotted relaxation curves for  $R_{AB} = 1.1$  and different values of  $(\gamma, \theta_{i,B})$ , specifically  $\gamma = 0.067$  and  $0.1$ , and  $\gamma\theta_{i,B} = 10$  and  $100$ .

Next, we look into the Kovacs effect. Therein, the system is first aged by letting it relax from  $T_i$  to  $T_1 < T_i$ . This relaxation towards the aging temperature  $T_1$  is interrupted at a certain waiting time  $t_w$ . Thereat, the system is put in contact with a thermal reservoir at temperature  $T_w$ ,  $T_w \equiv T(t_w)$ . The Kovacs effect emerges when, for  $t > t_w$ ,  $T(t)$  departs from its initial (and equilibrium) value and passes through a maximum before returning to  $T_w$ . In our system, it comes about because the cumulants are non-zero at the waiting time and, thus, to maximise the effect the (absolute) value of  $a_2$  and  $a_3$  have to be in turn maximised. This entails that the optimal protocol is a quench to a much lower temperature, i.e.  $T_1 \ll T_i$ , over which the system reaches the LLNES. Equations (5) govern the time evolution of the system for  $t > t_w$ , with  $\theta = T/T_w$  and initial conditions  $\theta(t_w) = 1$ ,  $a_2(t_w) = a_2^r$ ,  $a_3(t_w) = a_3^r$ .

The resulting Kovacs response also has universal prop-

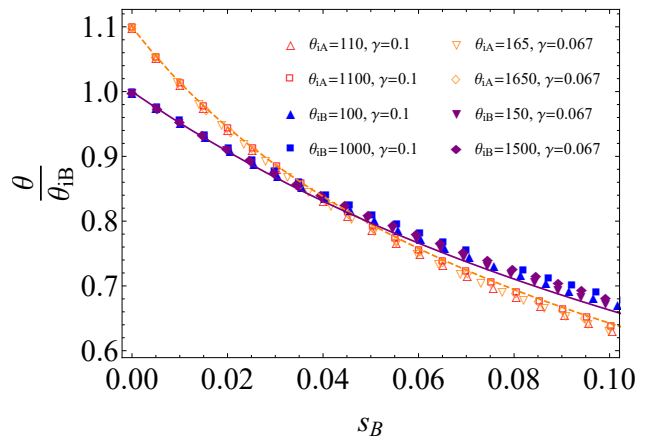


FIG. 3. Universal Mpemba effect for different initial preparations. In particular, we plot  $\theta/\theta_{i,B}$ , i.e. the temperature in units of the initial temperature of the colder sample, as a function of the scaled time  $s_B$  for the colder sample, defined in Eq. (10). For a fixed value of the initial temperature ratio  $R_{AB}$ , all the curves corresponding to different values of  $(\gamma, \theta_{i,B})$  superimpose, both for the hotter (A) (open symbols) and colder (B) samples (filled symbols). There are eight simulation curves: four corresponding to hot samples with  $R_{AB} = 1.1$  and the corresponding four curves for the cold samples. Dashed and full curves correspond to the solutions of Eq. (6) for  $(a_{2i}, a_{3i}) = (0, 0)$  and  $(a_2^r, a_3^r)$ , respectively.

erties: the initial conditions and, therefore, the subsequent Kovacs hump do not depend on  $(T_i, T_w, T_1)$ . Yet, it does depend on  $\gamma$ : in fact, it is roughly proportional to  $\gamma$  [56]. Figure 4 illustrates this universal Kovacs hump, we show the evolution of  $\theta = T/T_w$  as a function of  $t - t_w$ , for  $t > t_w$ . Indeed, the triplet  $(T_i, T_w, T_1)$  does not affect the Kovacs hump measured in DSMC simulations. Here, for the sake of simplicity, we have taken one of the aging temperatures as the unity of temperature [66]. Moreover, our theory quantitatively describes the numerical results: the agreement is very good, especially when the simulation value of  $a_2^r$  is employed [67].

*Conclusions.* - The molecular fluid with non-linear drag shows a very complex relaxation behaviour. The leading role in this behaviour is played by the LLNES that is reached by the system when quenched to a low temperature. Over it, the temperature displays a very slow, algebraic, decay and the VDF neatly separates from the Maxwellian shape. The strong non-Gaussianities are characterised by large (absolute) values of the fourth and sixth cumulants of the VDF,  $a_2^r$  and  $a_3^r$ , respectively.

This LLNES also rules the emergence of strong memory effects in the system, both for the Mpemba and the Kovacs effect. On the one hand, not only have we shown that a strong Mpemba effect (present for temperature differences up to 40 per cent) comes about but also how the hot and cold samples have to be prepared. The hot sample starts from equilibrium whereas the cold sample starts from the LLNES described above. On the other hand, it is the relaxation following the quench to a low

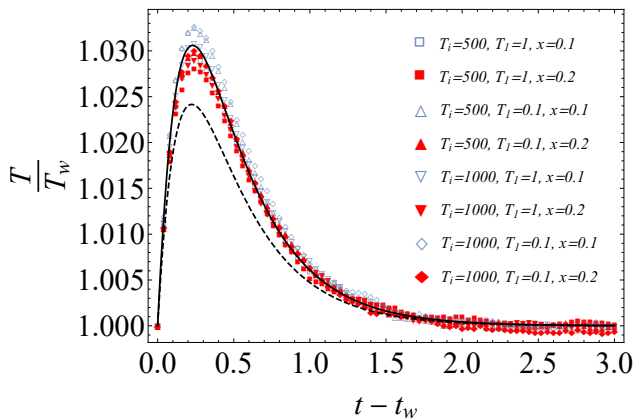


FIG. 4. Evolution of the temperature in the Kovacs protocol. Parameter values are  $\gamma = 0.1$ ,  $d = 2$ , and  $\xi = 1$ . Eight simulation curves are shown for different combinations of the initial ( $T_i$ ), aging ( $T_1$ ), and final temperature ( $T_w$ ). Writing the aging temperature as  $T_w = T_1 + x(T_i - T_1)$ , the data shown correspond to  $x = 0.2$  (filled symbols) and  $0.1$  (open symbols). Curves for smaller values of  $x$  are basically superimposed with those for  $x = 0.1$ . The dashed (solid) line corresponds to the numerical integration of Eqs. (5) with the theoretical (simulation) values for the cumulants over the LLNES.

temperature that has to be interrupted to maximise the Kovacs effect, once the system reaches the LLNES. The reported Kovacs hump, which is of the order of 3 per cent in Fig. 4, is quite strong as compared to typical values [68].

Both the non-exponential relaxation and the memory effects present universal features. When properly scaled, all the relaxation curves corresponding to the quench to a low temperature superimpose. For the Mpemba effect, a similar scaling entails that all the curves corresponding to a given initial temperature ratio also superimpose, independently of the value of other parameters: degree of non-linearity, and initial values of the temperatures of the hot and cold samples. The Kovacs effect also displays some universal properties, although they are somehow weaker: the hump depends on  $\gamma$  but not on the initial, final, and aging temperatures.

Our work opens the door to looking for aging phenomena and glassy behaviour in ultracold atoms. Specifically, the model employed here describes mixtures of ultracold atoms, like the system composed of Cs and Rb atoms considered in Ref. [55]. In this context, the key role played by the LLNES for the emergence of non-exponential relaxation and the associated memory effects (both Mpemba and Kovacs-like), which is a key result of this work, may be checked in real experiments.

#### ACKNOWLEDGMENTS

We acknowledge financial support from project PGC2018-093998-B-I00, funded by: FEDER/Ministerio de Ciencia e Innovación–Agencia Estatal de Investigación (Spain). A. Patrón acknowledges support from the FPU programme through Grant FPU2019-4110. Also, we would like to thank D. Guéry-Odelin, A. Megías and A. Santos for useful discussions.

- 
- [1] F. H. Stillinger and P. G. Debenedetti, Glass Transition Thermodynamics and Kinetics, *Annual Review of Condensed Matter Physics* **4**, 263 (2013).
  - [2] V. Lubchenko, Theory of the structural glass transition: a pedagogical review, *Advances in Physics* **64**, 283 (2015).
  - [3] S. R. Nagel, Experimental soft-matter science, *Reviews of Modern Physics* **89**, 025002 (2017).
  - [4] G. Williams and D. C. Watts, Non-symmetrical dielectric relaxation behaviour arising from a simple empirical decay function, *Trans. Faraday Soc.* **66**, 80 (1970).
  - [5] R. G. Palmer, D. L. Stein, E. Abrahams, and P. W. Anderson, Models of hierarchically constrained dynamics for glassy relaxation, *Physical Review Letters* **53**, 958 (1984).
  - [6] W. Kob and R. Schilling, Dynamics of a one-dimensional “glass” model: Ergodicity and nonexponential relaxation, *Physical Review A* **42**, 2191 (1990).
  - [7] J. J. Brey and A. Prados, Stretched exponential decay at intermediate times in the one-dimensional Ising model at low temperatures, *Physica A* **197**, 569 (1993).
  - [8] J. J. Brey and A. Prados, Low-temperature relaxation in the one-dimensional Ising model, *Physical Review E* **53**, 458 (1996).
  - [9] C. A. Angell, K. L. Ngai, G. B. McKenna, P. F. McMillan, and S. W. Martin, Relaxation in glassforming liquids and amorphous solids, *Journal of Applied Physics* **88**, 3113 (2000).
  - [10] J. J. Brey and A. Prados, Slow logarithmic relaxation in models with hierarchically constrained dynamics, *Physical Review E* **63**, 021108 (2001).
  - [11] R. Richert, Physical Aging and Heterogeneous Dynamics, *Physical Review Letters* **104**, 085702 (2010).
  - [12] K. Paeng, H. Park, D. T. Hoang, and L. J. Kaufman, Ideal probe single-molecule experiments reveal the intrinsic dynamic heterogeneity of a supercooled liquid, *Proceedings of the National Academy of Sciences* **112**, 4952 (2015).
  - [13] Y. Lahini, O. Gottesman, A. Amir, and S. M. Rubinstein, Nonmonotonic Aging and Memory Retention in Disordered Mechanical Systems, *Physical Review Letters* **118**, 085501 (2017).
  - [14] L. Kringle, W. A. Thornley, B. D. Kay, and G. A. Kimmel, Structural relaxation and crystallization in supercooled water from 170 to 260 K, *Proceedings of the National Academy of Sciences* **118**, e2022884118 (2021).
  - [15] Y. Nishikawa, M. Ozawa, A. Ikeda, P. Chaudhuri, and L. Berthier, Relaxation dynamics in the energy landscape

- of glass-forming liquids, arXiv:2106.01755 [cond-mat] .
- [16] A. J. Kovacs, Transition vitreuse dans les polymères amorphes. Etude phénoménologique, Fortschritte Der Hochpolymeren-Forschung **3**, 394 (1963).
- [17] A. J. Kovacs, J. J. Aklonis, J. M. Hutchinson, and A. R. Ramos, Isobaric volume and enthalpy recovery of glasses. II. A transparent multiparameter theory, Journal of Polymer Science: Polymer Physics Edition **17**, 1097 (1979).
- [18] A. Buhot, Kovacs effect and fluctuation–dissipation relations in 1d kinetically constrained models, Journal of Physics A: Mathematical and General **36**, 12367 (2003).
- [19] E. M. Bertin, J. P. Bouchaud, J. M. Drouffe, and C. Godrèche, The Kovacs effect in model glasses, Journal of Physics A: Mathematical and General **36**, 10701 (2003).
- [20] J. J. Arenzon and M. Sellitto, Kovacs effect in facilitated spin models of strong and fragile glasses, The European Physical Journal B-Condensed Matter and Complex Systems **42**, 543 (2004).
- [21] S. Mossa and F. Sciortino, Crossover (or Kovacs) effect in an aging molecular liquid, Physical Review Letters **92**, 045504 (2004).
- [22] G. Aquino, L. Leuzzi, and T. M. Nieuwenhuizen, Kovacs effect in a model for a fragile glass, Physical Review B **73**, 094205 (2006).
- [23] E. Bouchbinder and J. S. Langer, Nonequilibrium thermodynamics of the Kovacs effect, Soft Matter **6**, 3065 (2010).
- [24] G. Diezemann and A. Heuer, Memory effects in the relaxation of the Gaussian trap model, Physical Review E **83**, 031505 (2011).
- [25] M. Ruiz-García and A. Prados, Kovacs effect in the one-dimensional Ising model: A linear response analysis, Physical Review E **89**, 012140 (2014).
- [26] M. Lulli, C.-S. Lee, H.-Y. Deng, C.-T. Yip, and C.-H. Lam, Spatial Heterogeneities in Structural Temperature Cause Kovacs' Expansion Gap Paradox in Aging of Glasses, Physical Review Letters **124**, 095501 (2020).
- [27] I. L. Morgan, R. Avinery, G. Rahamim, R. Beck, and O. A. Saleh, Glassy Dynamics and Memory Effects in an Intrinsically Disordered Protein Construct, Physical Review Letters **125**, 058001 (2020).
- [28] L. Song, W. Xu, J. Huo, F. Li, L.-M. Wang, M. Ediger, and J.-Q. Wang, Activation Entropy as a Key Factor Controlling the Memory Effect in Glasses, Physical Review Letters **125**, 135501 (2020).
- [29] M. Peyrard and J.-L. Garden, Memory effects in glasses: Insights into the thermodynamics of out-of-equilibrium systems revealed by a simple model of the Kovacs effect, Physical Review E **102**, 052122 (2020).
- [30] R. Mandal, D. Tapias, and P. Sollich, Memory in Non-Monotonic Stress Response of an Athermal Disordered Solid, arXiv:2103.14766 [cond-mat] .
- [31] J.-P. Bouchaud, Weak ergodicity breaking and aging in disordered systems, Journal de Physique I **2**, 1705 (1992).
- [32] L. F. Cugliandolo and J. Kurchan, Analytical solution of the off-equilibrium dynamics of a long-range spin-glass model, Physical Review Letters **71**, 173 (1993).
- [33] A. Prados, J. J. Brey, and B. Sánchez-Rey, Aging in the one-dimensional Ising model with Glauber dynamics, EPL **40**, 13 (1997).
- [34] M. Nicodemi and A. Coniglio, Aging in out-of-equilibrium dynamics of models for granular media, Physical Review Letters **82**, 916 (1999).
- [35] S. R. Ahmad and S. Puri, Velocity distributions and aging in a cooling granular gas, Physical Review E **75**, 031302 (2007).
- [36] J. J. Brey, A. Prados, M. I. García de Soria, and P. Maynar, Scaling and aging in the homogeneous cooling state of a granular fluid of hard particles, Journal of Physics A: Mathematical and Theoretical **40**, 14331 (2007).
- [37] J. Parravicini, C. Conti, A. J. Agranat, and E. DelRe, Rejuvenation in scale-free optics and enhanced diffraction cancellation life-time, Optics Express **20**, 27382 (2012).
- [38] S. Dillavou and S. M. Rubinstein, Nonmonotonic Aging and Memory in a Frictional Interface, Physical Review Letters **120**, 224101 (2018).
- [39] E. B. Mpemba and D. G. Osborne, Cool?, Physics Education **4**, 172 (1969).
- [40] M. Baity-Jesi, E. Calore, A. Cruz, L. A. Fernandez, J. M. Gil-Narvión, A. Gordillo-Guerrero, D. Iñiguez, A. Lasanta, A. Maiorano, E. Marinari, V. Martin-Mayor, J. Moreno-Gordo, A. Muñoz Sudupe, D. Navarro, G. Parisi, S. Perez-Gaviro, F. Ricci-Tersenghi, J. J. Ruiz-Lorenzo, S. F. Schifano, B. Seoane, A. Tarancón, R. Tripiccion, and D. Yllanes, The Mpemba effect in spin glasses is a persistent memory effect, Proceedings of the National Academy of Sciences **116**, 15350 (2019).
- [41] Z. Lu and O. Raz, Nonequilibrium thermodynamics of the Markovian Mpemba effect and its inverse, Proceedings of the National Academy of Sciences **114**, 5083 (2017).
- [42] I. Klich, O. Raz, O. Hirschberg, and M. Vucelja, Mpemba Index and Anomalous Relaxation, Physical Review X **9**, 021060 (2019).
- [43] A. Gal and O. Raz, Precooling Strategy Allows Exponentially Faster Heating, Physical Review Letters **124**, 060602 (2020).
- [44] A. Kumar and J. Bechhoefer, Exponentially faster cooling in a colloidal system, Nature **584**, 64 (2020).
- [45] A. Lasanta, F. Vega Reyes, A. Prados, and A. Santos, When the Hotter Cools More Quickly: Mpemba Effect in Granular Fluids, Physical Review Letters **119**, 148001 (2017).
- [46] A. Torrente, M. A. López-Castaño, A. Lasanta, F. V. Reyes, A. Prados, and A. Santos, Large Mpemba-like effect in a gas of inelastic rough hard spheres, Physical Review E **99**, 060901 (2019).
- [47] A. Santos and A. Prados, Mpemba effect in molecular gases under nonlinear drag, Physics of Fluids **32**, 072010 (2020).
- [48] A. Biswas, V. V. Prasad, O. Raz, and R. Rajesh, Mpemba effect in driven granular Maxwell gases, Physical Review E **102**, 012906 (2020).
- [49] A. Biswas, V. V. Prasad, and R. Rajesh, Mpemba effect in an anisotropically driven granular gas, arXiv:2104.08730 [cond-mat] .
- [50] R. Gómez González, N. Khalil, and V. Garzó, Mpemba-like effect in driven binary mixtures, Physics of Fluids **33**, 053301 (2021).
- [51] S. Takada, H. Hayakawa, and A. Santos, Mpemba effect in inertial suspensions, Physical Review E **103**, 032901 (2021).
- [52] Y. L. Klimontovich, Nonlinear Brownian motion, Physics-Uspokhi **37**, 737 (1994).
- [53] L. Ferrari, Particles dispersed in a dilute gas: Limits of validity of the Langevin equation, Chemical Physics **336**, 27 (2007).

- [54] L. Ferrari, Particles dispersed in a dilute gas. II. From the Langevin equation to a more general kinetic approach, *Chemical Physics* **428**, 144 (2014).
- [55] M. Hohmann, F. Kindermann, T. Lausch, D. Mayer, F. Schmidt, E. Lutz, and A. Widera, Individual Tracer Atoms in an Ultracold Dilute Gas, *Physical Review Letters* **118**, 263401 (2017).
- [56] See the Supplemental Material at [URL will be inserted by publisher] for more details on the analytical calculations and additional figures.
- [57] For the ultracold gas mixture considered in Ref. [55],  $\xi \simeq 674$ .
- [58] In Ref. [47], the simpler first Sonine approximation of the kinetic equation, in which  $a_3$  is neglected, was employed to analytically investigate the Mpemba effect. However, this approximation fails to reproduce the dynamical behaviour observed in simulations [56].
- [59] A. Megías, A. Santos, and A. Prados, (in preparation).
- [60] In the three-dimensional case,  $\gamma = 0.1$  for self-diffusion (equal masses). For the ultracold gas mixture considered in Ref. [55],  $\gamma \simeq 0.067$ .
- [61] G. A. Bird, *Molecular Gas Dynamics and the Direct Simulation of Gas Flows* (Clarendon Press, Oxford, 1994).
- [62] J. M. Montanero and A. Santos, Monte Carlo simulation method for the Enskog equation, *Physical Review E* **54**, 438 (1996).
- [63] For the values of the parameters in Fig. 1, this takes place for very small values of  $\theta/\theta_i$ , namely  $\theta/\theta_i \lesssim 0.04$  ( $1/Y \gtrsim 25$ ).
- [64] A similar tendency of the cooling rate with the excess kurtosis has been found in other systems described at a kinetic level, both with inelastic and elastic collisions [45–47, 50, 51].
- [65] For  $\gamma = 0.1$ , it is  $a_2^{\max} \simeq 0.04$ , which is an order of magnitude smaller than  $a_2^r$ . Thus, this choice provides us with a difference  $a_{2i,A} - a_{2i,B}$  that is around 90 per cent of its maximum value.
- [66] In the relaxation experiment and the Mpemba memory effect, the unit of temperature was formally the steady temperature  $T_s$ .
- [67] Our theory underestimates  $a_2^r$  by roughly 15 per cent [56].
- [68] For example, it is one of order of magnitude larger the original observation by Kovacs [16, 17], 2–3 times larger than its value in a Lennard-Jones fluid [21], and of the same order of magnitude of the recently reported results in a disordered protein construct [27].